Determination of Carrier Diffusion Length using Transient Electron Photoemission Microscopy in the GaAs/InSe Heterojunction

Emilio J. Juarez-Perez*, Yabing Qi

Energy Materials and Surfaces Science Unit (EMSSU), Okinawa Institute of Science and Technology Graduate University, 1919-1 Tancha, Onna-son, Kunigami, Okinawa 904-495, Japan.

Key words: Diffusion Length, Time Resolve Photoemission Electron Microscopy, Charge Transport, Lifetime, InSe, GaAs Solar Cells

* Corresponding author: e-mail ejjuarezperez@gmail.com

Carrier diffusion lengths and lifetime parameters for electron transport filmed at nanoscale semiconductor slabs have been fitted using a 1D-model and decay data extracted from transient photoemission electron microscopy. Meanwhile a conventional photoluminescence quenching measurement needs two separate samples with an active material between blocking and quenching layers to characterize carrier transport properties. In this work, only one few layer mono-crystalline sample of γ-InSe containing different thicknesses of active material is used to obtain a common diffusion coefficient consistent with previously reported values for vertical carrier diffusion in layered InSe.

Copyright line will be provided by the publisher

1 Introduction Carrier diffusion length (L_D) is defined as the average distance that carriers are able to move through the semiconductor material before annihilated by recombination. L_D is one of the most important properties to consider during the design of any semiconductor based device. Therefore, an accurate determination of this parameter helps to characterize carrier transport properties ascribed to the semiconductor material under consideration.[1, 2]

Recently, 2D semiconductor layered heterostructures have received considerable attention because of their special structural anisotropy is neatly transferred into anisotropy for the carrier transport properties. This asymmetric transport feature could have potential to be exploited in novel applications. Besides, weak van der Waals interactions joining the layers of these 2D materials facilitates their exfoliation allowing the stack of different layered materials regardless of lattice mismatch, which is an attractive feature from the point of view of device fabrication.[3–8] 2D γ-InSe phase few layers semiconductor material found application as active material for photodetectors.[9–12] These photodetectors have demonstrated recently exceptional fast response speed, high photoresponsivity and a remarkable broad spectral range available for detection.[13–16] Layered semiconductors or van der Waals solids as for example 2D γ-InSe phase, have two channels for carrier transport, the so-called vertical transport/interplanar transport between layers of material and the horizontal/intraplanar transport. The latter is usually found 10-1000 times faster channel for carrier transport than interplanar transport.[17–21] Although experimental techniques accounting few layers of bulk InSe have demonstrated a slower intraplanar diffusion.[22] Noteworthy,to meet the challenges of further application of 2D heterostructures exploiting this transport anisotropy, a full separated vertical and planar carrier transport characterization method could be interesting for few layer 2D materials based heterojunctions.

Ambipolar carrier and exciton transport properties are usually assessed using time-resolved photoluminescence (TR-PL) measurements. Photoluminiscence quenching measurements have been previously used within hy-

Copyright line will be provided by the publisher

brid perovskite layer semiconductors[23–28], quantum dots[29], dyes[30] and organic bulk heterojunctions based solar cells[31, 32] in order to determine L_D of carriers independently if such carrier could be considered of excitonic nature (as in organic bulk heterojunctions) or weakly bound excitons almost free charge carriers (as in hybrid perovskites). A TR-PL based carrier transport determination in semiconductor thin-films implies to compare the different lifetime observed for carriers recombining radiatively between two asymmetric devices. A device consists of semiconductor layer with one side able to extract electron or hole carriers and another device with the semiconductor layer blocked in both sides. The difference in decay rate observed between both devices is attributed to diffusive carrier transport in the one-side quenched device. Importantly, TR-PL captures only the decay of carrier population recombining radiatively. Sometimes this carrier population is not a majority carrier in the material which usually (if not always) has larger carrier population undergoing non-radiative recombination.[33] Instead, time resolved photoemission electron microscopy (TR-PEEM) based measurement could be able to characterize transport for virtually "all" electron emission decays observed at the surface of nanoscale sized samples. Remarkably, the source of decay data is one of the most relevant differences between both techniques also as higher space and time resolution.

In this report, L_D parameters are extracted from experimental TR-PEEM decay data at the sub-nanosecond scale (from 0.8 to 100 ps) for the GaAs (intrinsic) /InSe (n-doped) heterojunction.[34] A diffusion-only non-stationary 1D model is proposed to simulate the TR-PEEM decay experiments and suitability of this model to extract the vertical diffusion coefficient (D_z), L_D and experimental lifetime parameters (τ) is discussed.

2 Theory

2.1 Preamble The InSe/GaAs heterostructures were produced by depositing an exfoliated flake of 2D γ-InSe onto an intrinsic GaAs wafer.[34] TR-PEEM decay data were collected from three different thickness zones on this InSe flake and also from free GaAs wafer. A scheme depicting the heterojunction is shown in Figure 1.a. The model applied in this heterojunction is one-dimensional and explicit in diffusion transport through z-axis. The lateral carrier diffusion transport (xy-plane) is implicitly considered as discussed below.

The band energy levels for this type II heterojunction (Figure 1.b) predicts a drift transport flow of photoexcited electrons from the GaAs wafer substrate $N_{0,GaAs}$ into the InSe slab containing its own photoexcited electron population $N_{0,InSe}$. The time dependent carrier injection rate from GaAs into InSe starting just after the 800 nm light pump pulse is assumed to be the same perfect injection from GaAs to InSe independently of thickness because the InSe flake share the same common bottom surface lying on the GaAs wafer. It is assumed that there is negligible photon attenuation reaching GaAs wafer due to nanosized thickness of the InSe slab and its low absorption coefficient at 800 nm wavelength. Once photoexcited electrons crossed the heterojunction, it is assumed that the experimental time dependent electron population decay observed in the extrinsic n-doped InSe slab is governed by diffusion and recombination with the minority carrier (holes).[35] Meanwhile, the majority carrier flux (electrons) arises from the built-in internal field, the minority carrier flux (holes) is exclusively due to the diffusion by carrier concentration gradients and diffusion coefficient. Because, the electroneutrality condition has to be satisfied for all points in the system, it implies that the ambipolar diffusion coefficient obtained for the extrinsic InSe slab is inherently a hole diffusion.

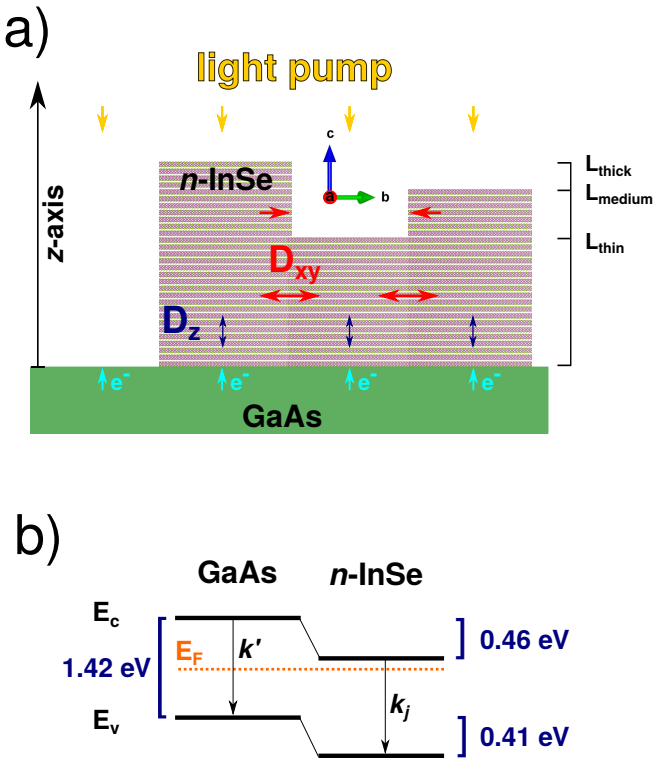

Figure 1 a) GaAs/InSe type II heterojunction with three different InSe thicknesses deposited on top of the GaAs substrate surface. The diffusion one-dimensional model is applied along the z-axis. The layered InSe model in the scheme provides thicknesses at z scale from InSe crystalline structure.[36] b) Band energy levels for this type II heterojunction using information from reference [34]

.

2.2 One-dimensional non-stationary diffusion-only model A finite-difference time-domain and one dimensional diffusion-only model to simulate the TR-PEEM decay experiments can be established using the non sta-

Copyright line will be provided by the publisher

tionary 1D diffusion differential equation of continuity as follows,

$$\frac{\partial n_j(z,t)}{\partial t} = D_z \frac{\partial^2 n_j(z,t)}{\partial z^2} - k_j(t) n_j(z,t) \tag{1}$$

where $n_j(z,t)$ (nm^{-1}) is the spatial and time dependent distribution of 1D carrier density in the InSe flake of j thickness (j : thick = 25, medium = 21.6 and thin = 16 nm), z (nm) is the independent space variable axis normal to the main plane in the slab and parallel to the c axis of the layered InSe, D_z (nm^2 ns^{-1}) is the vertical (interplanar) diffusion coefficient of the carriers (holes) and $k_j(t)$ (ns^{-1}) is a time dependent natural monomolecular recombination of the carriers for each InSe slab thickness following the differential form of the unimodal Berberan-Santos (BS) generalized decay equation. This generalized decay is able to describe an useful parametric switchable behavior on decays based in mono-exponential, modified stretched exponential, compressed hyperbola or even a mixed decay from all of them.[37]

Equation 1 needs one initial condition and two boundary conditions to be integrated. A step-function initial condition is established as,

$$n_j(z,0) = \begin{cases} N_{0,GaAs} & z = 0 \\ \frac{N_{0,InSe} \mathrm{e}^{(-\alpha(L_j - z))}}{L_j} & z > 0 \end{cases} \tag{2}$$

where $N_{0,GaAs}$ and $N_{0,InSe}$ are initial carrier density in the GaAs material and InSe at $t = 0$ just after light pump pulse, respectively. α is the linear InSe absorption coefficient at 800 nm wavelength parallel to the c-axis (α =$\sim$1800 cm^{-1})[18, 38]. L_j (j : thick, medium, thin) are the three thicknesses studied mentioned above. The expression $\frac{N_{0,InSe} e^{-\alpha(L_j - z)}}{L_j}$ describes the initial carrier density distribution in the j InSe slab depending on z, α and illuminated side of the sample. A stationary PL measurement showed a quantum efficiency photoluminescence ratio for InSe/GaAs of 2.71.[34] Then, it can be approximated that the initial relative total population of photoexcited carriers in the InSe flake ($N_{0,InSe}$) after light perturbation follows next relation,

$$N_{0,InSe} = \gamma \cdot N_{0,GaAs} \tag{3}$$

where γ is an empirical parameter containing information about PL quantum efficiency and flake/wafer shape factor.

The boundary condition in the InSe flake free side at $z = L$ (top side) is set as a Neumann type boundary condition considering that there is a blocking layer in such slab/vacuum interface,

$$\frac{\partial n_j(z,t)}{\partial z}\Big|_{z=L_j} = 0 \tag{4}$$

On the other hand, the boundary condition in the GaAs/InSe interface at $z = 0$ is set as a Robin type boundary condition considering a time dependent carrier injection rate from GaAs into InSe starting just after the 800 nm light pump pulse. This time dependent or dynamic injection rate is obtained assuming perfect injection from GaAs to InSe slab as,

$$\frac{\partial n_j(z,t)}{\partial z}\Big|_{z=0} = -k'(t) n_j(z,t) \tag{5}$$

where $k'(t)$ is obtained using eq. no. 6 and the TR-PEEM intensity decay observed in the GaAs substrate surface free of InSe quenching layer, see Figure 2.a.

$$k'(t) = -\frac{dN_{GaAs}/dt}{N_{GaAs}} \tag{6}$$

The differential algebraic system of equations obtained from (1) under initial (2) and boundary conditions (4,5) is solved simultaneously for all three InSe thicknesses L_j with their corresponding kinetic equation describing recombination and lifetime parameter $k_j(t)$ as fitting parameters and sharing a common diffusion coefficient D_z for all thicknesses. D_z and $k_j(t)$ are obtained in an iterative procedure minimizing the square difference between theoretical decay data obtained as,

$$N_j(t) = \int^{L_j} n_j(z,t) dz \tag{7}$$

and the experimental TR-PEEM decay data from reference [34]. L_D is obtained as,

$$L_D = \sqrt{D \cdot \tau_j} \tag{8}$$

where the lifetime (τ_j) for each thickness is calculated depending of the expression defining $k_j(t)$.

3 Methods The 1D model and iterative procedure code was implemented using MATLAB and deposited in GITHUB.[39] Experimental TR-PEEM surface data were collected from a previous work for three different InSe thicknesses and GaAs substrate surface.[34]

4 Results & Discussion Experimental and theoretical data points obtained using the 1D diffusion model are shown in Figure 2(b). Fitted parameters are summarized in Table 1. Figure 3 shows the calculated time-space carrier concentration $n(z,t)$ and diffusive flux J_{diff} distribution for all InSe thicknesses studied using fitted parameters.

The diffusion-only model implemented in this work describes well the observed TR-PEEM surface decays for all InSe thicknesses. Large and medium InSe layer thickness follow a mono-exponential time independent recombination decay ($k_j(t) = 1/\tau_j$). However, the thinner InSe layer indicates a relevant modified stretched exponential behavior with $\beta = 0.60$ at longer times. Lifetimes τ_j are distributed on three order of magnitude from 1.87 $\cdot 10^{-3}$ to 4.14 $\cdot 10^{-1}$ ns. D_z was obtained self-consistently for all thicknesses as 2274 nm^2/ns ($\sim$0.023 cm^2/s). L_D is obtained using eq. 8 considering the different τ_j for each

Copyright line will be provided by the publisher

Table 1 Simulation parameters* for diffusion-only model.

InSe thickness (nm)	τ_j (ns)	Decay type	RMSD† (C)	D_z (nm^2 ns^{-1})	L_D (nm)
25	$(4.14 \pm 0.06)\cdot 10^{-1}$	mono-exponential	$5.06\cdot 10^{-4}$		30.7 ± 1.3
21.6	$(3.55 \pm 0.09)\cdot 10^{-2}$	mono-exponential	$2.12\cdot 10^{-4}$	2274 ± 30	8.98 ± 0.16
16	$(1.87 \pm 0.05)\cdot 10^{-3}$	strechted exponential ($\beta = 0.60^{\sharp}$)	$2.01\cdot 10^{-4}$		2.06 ± 0.04

*Confidence interval at 95 % for fitting parameters obtained by bootstrapping 100 random trials of experimental data.
†Square root of the mean of the squares of the deviations between experimental and theoretical data in C units: RMSD $_j = q \cdot \sqrt{\frac{\sum_{t=1}^{k}(N_{model,j} - N_{exp,j})^2}{k}}$ where q is the elemental charge constant.
♯ Shape-defining β dimensionless parameter for BS equation[37] used to switch easily between mono-exponential ($\beta = 1$, $\forall\sigma \in (0,1)$) or compressed hyperbolic ($\beta = 0$, $\forall\sigma \in (0,1)$) or modified stretched exponential decay (σ =1 and $\beta > 0$).

thickness. It is found that only the thicker InSe slab has a L_D larger than its physical thickness sustaining the largest surface photoemission for the longest time.

In principle, this counterintuitive effect can be explained assuming that thinner zones of InSe suffers a higher recombination rate due to higher carrier concentration. Alternatively, the thinner zones are more exposed to intraplanar diffusion D_{xy} than thicker zones because the three modeled thicknesses share a common surface lying into the GaAs wafer (see Figure 1.a). In this way, the kinetic term in equation 1 could be capturing not only the recombination process but including implicitly intraplanar D_{xy} diffusion in the InSe slab.

InSe is a layered material and a large anisotropy of the electronic properties is obtained depending of the crystallographic axis considered for carrier transport. Our D_z obtained from fittings is equivalent to $\sim$0.9 cm^2/(V s) of carrier mobility using the Einstein relation at 298K. This mobility agrees well with hole mobilities (minority carrier in n-doped InSe) reported in literature for InSe interlayer mobility along the c-axis.[17, 40] It validates the usefulness of surface TR-PEEM decay data and this model to extract relevant parameters characterizing vertical (interplanar) carrier transport.

A comparison between the only-drift model included in ref. [34] and the only-diffusion model presented here reveals that there is a good agreement between the three τ_j fitted lifetime parameters for each InSe thickness, see Table 2. It reinforces the idea that such τ_j are capturing implicitly the large intraplanar diffusion (D_{xy}) in the InSe layered material. There is a clear advantage using a diffusion-only based model solving self-consistently a common vertical diffusion coefficient D_z parameter for all material thicknesses because the fundamental parameter L_D can be obtained using equation 8 for the specific shape, orientation and dimensions of the system. Furthermore, applying diffusion-only model would avoid to estimate a common drift velocity for all thicknesses as $v_{drift} = \mu\mathcal{E} = \frac{q\tau}{m_e^*}\frac{d\phi}{dz}$ guessing scattering time (τ) and to collect reduced electron effective constants parameters (m_e^*) from literature to apply the drift model.

Table 2 Lifetimes fitted for different thicknesses using drift-only and diffusion-only models

L_j (nm)	τ_j (ns)	
	Drift-only†	Diffusion-only*
thick	$5.00\cdot 10^{-1}$	$4.14\cdot 10^{-1}$
medium	$4.36\cdot 10^{-2}$	$3.55\cdot 10^{-2}$
thin	$3.12\cdot 10^{-3}$	$1.87\cdot 10^{-3}$

†Man et al.[34] *This work.

5 Conclusion Retrieval of the interplanar carrier diffusion in van der Waals stacked structures is challenging. In this work, a set of space and time resolved photoemission electron microscopy (TR-PEEM) surface decay data obtained at the GaAs/InSe heterojunction were fitted using a finite-difference time-domain and vertical one dimensional diffusion-only model including a dynamic carrier injection boundary condition. The vertical diffusion coefficient D_z was constrained during the global fitting to obtain self-consistently a value independent of InSe thickness but allowing freedom in the kinetics describing carrier recombination for all different InSe thicknesses simultaneously. The plasticity of the Berberan-Santos generalized decay function applied in the recombination term could collect a super/supra exponential behavior ascribed implicitly to intraplanar diffusion D_{xy} besides the usual recombination rate term. Diffusion length L_D obtained for each thickness indicates that only the largest InSe layer thickness has a diffusion length larger than its physical material thickness. Derived carrier mobility for InSe agrees well with hole mobilities (minority carrier in n-doped InSe) reported in literature for InSe interlayer (vertical) mobility along the c-axis.

Acknowledgements Authors thank Michael K. L. Man and Prof. Keshav M. Dani for providing the experimental data of Figure 4c in ref.[34]. E.J.J-P. acknowledges the funding support from JSPS KAKENHI Grant Number 17K14551. Y.B.Q. acknowledge the funding support from the Energy Materials and Surface Sciences Unit of the Okinawa Institute of Science and Technology Graduate University, the OIST Proof of Concept

Copyright line will be provided by the publisher

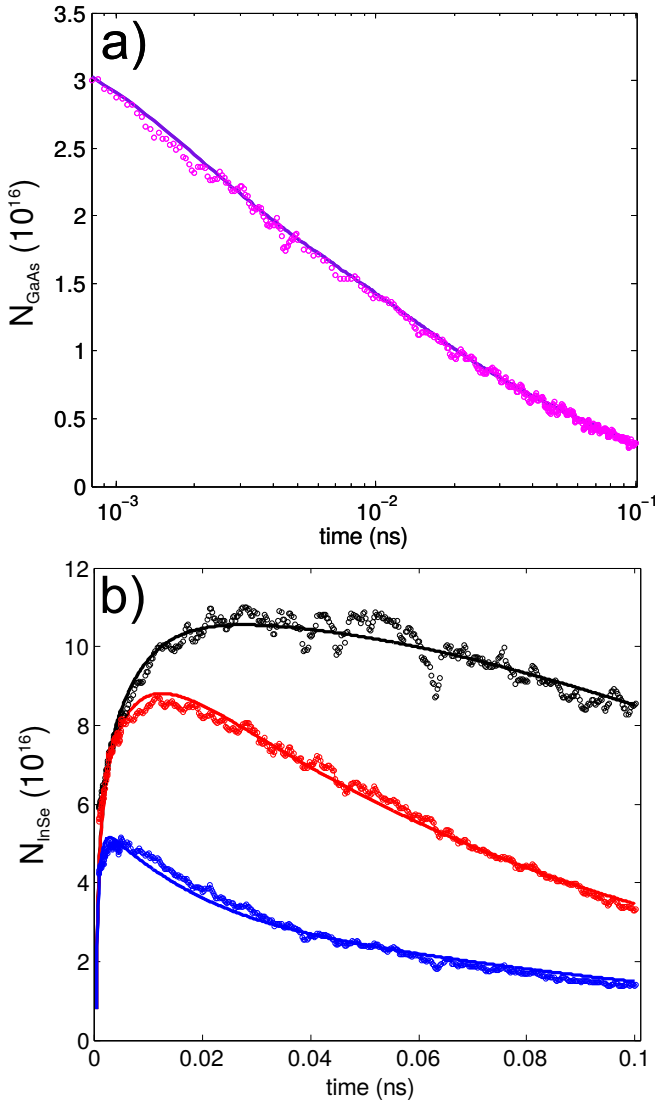

Figure 2 a) Experimental TR-PEEM decay (pink circles) from free InSe GaAs surface substrate and triexponential unsconstrained fitting function (blue line). b) Experimental TR-PEEM surface data (o) and model data (solid line) predicted using a diffusion-only model for thick (black), medium (red) and thin (blue) InSe slab thicknesses.

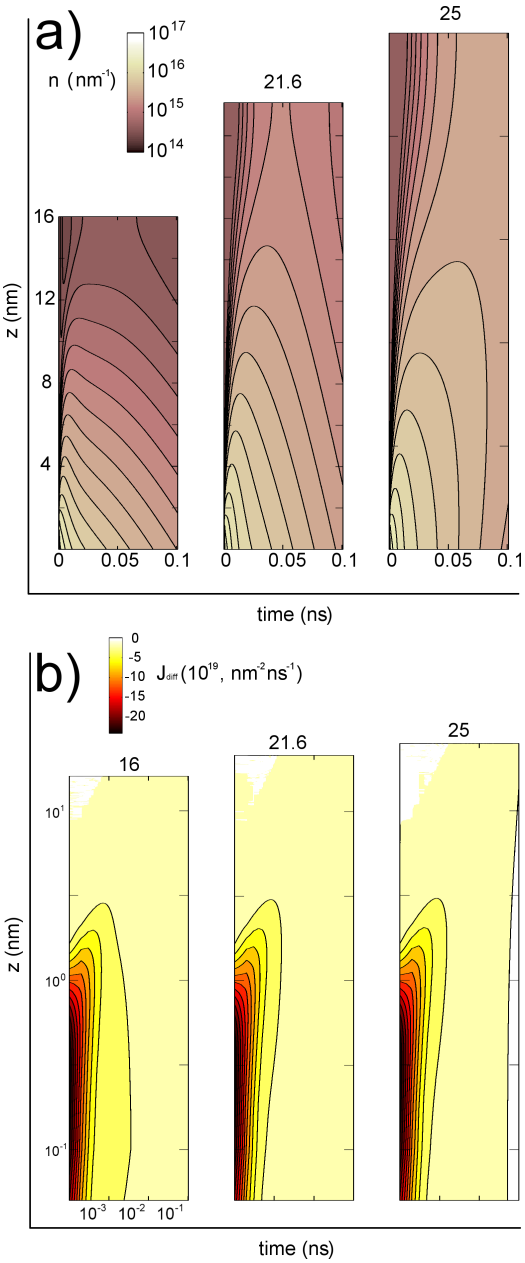

Figure 3 Calculated a) $n(z,t)$ and b) J_{diff} distribution (y and x axis in log scale) for all InSe thicknesses using parameterized D_z and τ_j obtained after fitting.

(POC) Program, the OIST R&D Cluster Research Program, and JSPS KAKENHI Grant Number JP18K05266.

References

[1] G. Hodes, P. V. Kamat, *J. Phys. Chem. Lett.*, **2015**, *6*, 4090.
[2] S. Sze, *Semiconductor Devices. Physics and Technology 2nd Edition*, John Wiley & Sons, 2002.
[3] L. Huang, N. Huo, Y. Li, H. Chen, J. Yang, Z. Wei, J. Li, S.-S. Li, *J. Phys. Chem. Lett.*, **2015**, *6*, 2483.
[4] Y. Deng, Z. Luo, N. J. Conrad, H. Liu, Y. Gong, S. Najmaei, P. M. Ajayan, J. Lou, X. Xu, P. D. Ye, *ACS Nano*, **2014**, *8*, 8292.
[5] G. W. Shim, K. Yoo, S.-B. Seo, J. Shin, D. Y. Jung, I.-S. Kang, C. W. Ahn, B. J. Cho, S.-Y. Choi, *ACS Nano*, **2014**, *8*, 6655.

Copyright line will be provided by the publisher

[6] S. Zhang, M. Xie, F. Li, Z. Yan, Y. Li, E. Kan, W. Liu, Z. Chen, H. Zeng, *Angew. Chem., Int. Ed.*, **2016**, *55*, 1666.
[7] J. Kang, S. A. Wells, V. K. Sangwan, D. Lam, X. Liu, J. Luxa, Z. Sofer, M. C. Hersam, *Adv. Mater.*, **2018**, *30*, 1802990.
[8] M. Hamer, E. Tóvári, M. Zhu, M. D. Thompson, A. Mayorov, J. Prance, Y. Lee, R. P. Haley, Z. R. Kudrynskyi, A. Patanè, D. Terry, Z. D. Kovalyuk, K. Ensslin, A. V. Kretinin, A. Geim, R. Gorbachev, *Nano Lett.*, **2018**, *18*, 3950.
[9] S. R. Tamalampudi, Y.-Y. Lu, R. K. U., R. Sankar, C.-D. Liao, K. M. B., C.-H. Cheng, F. C. Chou, Y.-T. Chen, *Nano Lett.*, **2014**, *14*, 2800.
[10] X. Wei, F.-G. Yan, C. Shen, Q.-S. Lv, K.-Y. Wang, *Chin. Phys. B*, **2017**, *26*, 038504.
[11] F. Yan, Z. Wei, X. Wei, Q. Lv, W. Zhu, K. Wang, *Small Methods*, **2018**, *2*, 1700349.
[12] Z. Yang, W. Jie, C.-H. Mak, S. Lin, H. Lin, X. Yang, F. Yan, S. P. Lau, J. Hao, *ACS Nano*, **2017**, *11*, 4225.
[13] W. Luo, Y. Cao, P. Hu, K. Cai, Q. Feng, F. Yan, T. Yan, X. Zhang, K. Wang, *Adv. Opt. Mater.*, **2015**, *3*, 1418.
[14] F. Yan, L. Zhao, A. Patanè, P. Hu, X. Wei, W. Luo, D. Zhang, Q. Lv, Q. Feng, C. Shen et al., *Nanotechnology*, **2017**, *28*, 27LT01.
[15] G. W. Mudd, S. A. Svatek, L. Hague, O. Makarovsky, Z. R. Kudrynskyi, C. J. Mellor, P. H. Beton, L. Eaves, K. S. Novoselov, Z. D. Kovalyuk, E. E. Vdovin, A. J. Marsden, N. R. Wilson, A. Patanè, *Adv. Mater.*, **2015**, *27*, 3760.
[16] S. Lei, F. Wen, L. Ge, S. Najmaei, A. George, Y. Gong, W. Gao, Z. Jin, B. Li, J. Lou, J. Kono, R. Vajtai, P. Ajayan, N. J. Halas, *Nano Lett.*, **2015**, *15*, 3048.
[17] A. Segura, J. Guesdon, J. Besson, A. Chevy, *J. Appl. Phys.*, **1983**, *54*, 876.
[18] B. Theys, *Revue Phys. Appl.*, **1988**, *23*, 1375.
[19] S. Sucharitakul, N. J. Goble, U. R. Kumar, R. Sankar, Z. A. Bogorad, F.-C. Chou, Y.-T. Chen, X. P. A. Gao, *Nano Lett.*, **2015**, *15*, 3815.
[20] P.-H. Ho, Y.-R. Chang, Y.-C. Chu, M.-K. Li, C.-A. Tsai, W.-H. Wang, C.-H. Ho, C.-W. Chen, P.-W. Chiu, *ACS Nano*, **2017**, *11*, 7362.
[21] M. Li, C.-Y. Lin, S.-H. Yang, Y.-M. Chang, J.-K. Chang, F.-S. Yang, C. Zhong, W.-B. Jian, C.-H. Lien, C.-H. Ho, H.-J. Liu, R. Huang, W. Li, Y.-F. Lin, J. Chu, *Adv. Mater.*, **2018**, *30*, 1803690.
[22] C. Zhong, V. K. Sangwan, J. Kang, J. Luxa, Z. Sofer, M. C. Hersam, E. A. Weiss, *J. Phys. Chem. Lett.*, **2019**, *10*, 493.
[23] S. D. Stranks, G. E. Eperon, G. Grancini, C. Menelaou, M. J. P. Alcocer, T. Leijtens, L. M. Herz, A. Petrozza, H. J. Snaith, *Science*, **2013**, *342*, 341.
[24] A. Listorti, E. J. Juarez-Perez, C. Frontera, V. Roiati, L. Garcia-Andrade, S. Colella, A. Rizzo, P. Ortiz, I. Mora-Sero, *J. Phys. Chem. Lett.*, **2015**, *6*, 1628.
[25] P.-W. Liang, C.-C. Chueh, X.-K. Xin, F. Zuo, S. T. Williams, C.-Y. Liao, A. K.-Y. Jen, *Adv. Energy Mater.*, **2015**, *5*, 1400960.
[26] Y. Li, W. Yan, Y. Li, S. Wang, W. Wang, Z. Bian, L. Xiao, Q. Gong, *Sci. Rep.*, **2015**, *5*, 14485.
[27] C. La-o-vorakiat, T. Salim, J. Kadro, M.-T. Khuc, R. Haselsberger, L. Cheng, H. Xia, G. G. Gurzadyan, H. Su, Y. M. Lam, R. A. Marcus, M.-E. Michel-Beyerle, E. E. M. Chia, *Nat. Commun.*, **2015**, *6*, 7903.
[28] L. Ma, F. Hao, C. Stoumpos, B. Phelan, M. Wasielewski, M. Kanatzidis, *J. Am. Chem. Soc.*, **2016**, *138*, 14750.
[29] E. M. Lee, W. A. Tisdale, *J. Phys. Chem. C*, **2015**, *119*, 9005.
[30] S. E. Koops, B. C. O'Regan, P. R. Barnes, J. R. Durrant, *J. Am. Chem. Soc.*, **2009**, *131*, 4808.
[31] P. E. Shaw, A. Ruseckas, I. D. Samuel, *Adv. Mater.*, **2008**, *20*, 3516.
[32] R. R. Lunt, N. C. Giebink, A. A. Belak, J. B. Benziger, S. R. Forrest, *J. Appl. Phys.*, **2009**, *105*, 053711.
[33] I. Levine, S. Gupta, A. Bera, D. Ceratti, G. Hodes, D. Cahen, D. Guo, T. J. Savenije, J. Ávila, H. J. Bolink et al., *J. Appl. Phys.*, **2018**, *124*, 103103.
[34] M. K. Man, A. Margiolakis, S. Deckoff-Jones, T. Harada, E. L. Wong, M. B. M. Krishna, J. Madéo, A. Winchester, S. Lei, R. Vajtai, P. M. Ajayan, K. M. Dani, *Nat. Nanotechnol.*, **2017**, *12*, 36.
[35] J. P. McKelvey, *Solid State And Semiconductor Physics*, Robert E. Krieger Publishing Company, 1984.
[36] A. Likforman, D. Carre, J. Etienne, B. Bachet, *Acta Crystallogr., Sect. B: Struct. Crystallogr. Cryst. Chem.*, **1975**, *31*, 1252.
[37] M. N. Berberan-Santos, *Chem. Phys. Lett.*, **2008**, *460*, 146.
[38] M. Andriyashik, M. Sakhnovskii, V. Timofeev, A. Yakimova, *Phys. Status Solidi B*, **1968**, *28*, 277.
[39] E. J. Juarez-Perez, Trpl-pvk, `https://github.com/ej-jp/TRPL-PVK`, 2018.
[40] M. D. Giulio, G. Micocci, A. Rizzo, A. Tepore, *J. Appl. Phys.*, **1983**, *54*, 5839.

Copyright line will be provided by the publisher

Graphical Table of Contents

GTOC image:

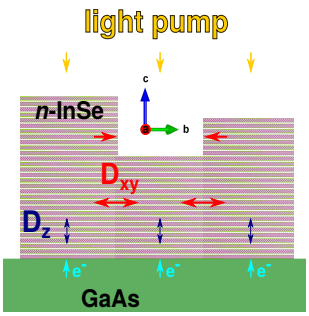

Transient photoemission electron microscopy decay data in the GaAs/InSe heterojunction is used for carrier diffusion length modeling. The derived vertical carrier mobility is consistent with interlayer hole mobility in γ-InSe.

Copyright line will be provided by the publisher